

RSC Advances



This is an *Accepted Manuscript*, which has been through the Royal Society of Chemistry peer review process and has been accepted for publication.

Accepted Manuscripts are published online shortly after acceptance, before technical editing, formatting and proof reading. Using this free service, authors can make their results available to the community, in citable form, before we publish the edited article. This *Accepted Manuscript* will be replaced by the edited, formatted and paginated article as soon as this is available.

You can find more information about *Accepted Manuscripts* in the [Information for Authors](#).

Please note that technical editing may introduce minor changes to the text and/or graphics, which may alter content. The journal's standard [Terms & Conditions](#) and the [Ethical guidelines](#) still apply. In no event shall the Royal Society of Chemistry be held responsible for any errors or omissions in this *Accepted Manuscript* or any consequences arising from the use of any information it contains.



Journal Name

ARTICLE

Insights into the binding of photothermal therapeutic agent bismuth sulfide nanorods with human serum albumin

Selvaraj Naveenraj^{a,b}, Ramalinga Viswanathan Mangalaraja^{a*}, Jerry J. Wu^c, Abdullah M. Asiri^d, Sambandam Anandan^{b**}

Received 00th January 20xx,
Accepted 00th January 20xx

DOI: 10.1039/x0xx00000x

www.rsc.org/

The biomedical application of bismuth sulfide (Bi_2S_3) nanorods as nanomedicine for the photothermal therapy of tumor leads to investigate their interaction with human serum albumin (HSA) to understand their pharmacokinetics. Hence, Bi_2S_3 nanorods with orthorhombic crystalline structure were synthesized using a simple microwave irradiation method using bismuth nitrate, sodium sulfide, and starch in aqueous medium. Thus synthesized Bi_2S_3 nanorods were well-characterized along with the investigation of their formation mechanism using powder X-ray diffraction (XRD), high-resolution transmission electron microscopy (HRTEM), selected area electron diffraction (SAED), and energy-dispersive X-ray (EDX). The interaction of Bi_2S_3 nanorods with HSA was investigated using absorption spectroscopy, fluorescence spectroscopy and circular dichroism spectroscopy. The absorption and time-resolved fluorescence spectroscopic studies confirmed that Bi_2S_3 nanorods interacted with HSA through static mechanism. The steady-state and the synchronous fluorescence spectral studies showed that the single binding site is near the tryptophan moiety (Trp-214) in HSA. The moderate binding constant determined from the steady-state fluorescence study suggests the possibility of effective transportation of Bi_2S_3 nanorods inside the body. These results could be a very helpful to understand the mechanisms and pathways responsible for the uptake, distribution and catabolism of Bi_2S_3 nanorods in multiple tissues of human body.

1. Introduction

Semiconductor nanomaterials are obtaining an overwhelming attention for their potential applications especially in the fabrication of optical and electronic devices within the past three decades.¹ Of which, Bismuth sulfide (Bi_2S_3), semiconductor with low toxicity and low direct band gap,²⁻⁴ has attracted considerable interest due to its potential applications in thermoelectric devices, electronic devices, optoelectronic devices, electrochemical hydrogen storage, hydrogen sensors, biosensors, photocatalytic hydrogen production, photocatalytic degradation, supercapacitors and biomolecular detection.⁶⁻¹⁰ One-Dimensional (1-D) nanostructured Bi_2S_3 materials such as nanorods, nanotubes, nanoribbons, nanocables and nanowires, have raised considerable interests due to their unusual properties facilitating the efficient electron transfer and potential uses in

the development of nanodevices.¹¹⁻¹³ To synthesize 1-D Bi_2S_3 nanostructures, many techniques including single source precursor method, evaporation route, thermal decomposition, hydrothermal method, solvothermal route, solventless thermolysis method, biomolecule-assisted approach, microwave irradiation, sonochemical method and template route have been utilized.^{12,14,15} Among them, microwave irradiation synthesis approach has more advantages such as shorter reaction time, higher reaction rate, more selective products with high yield, easy controllability, and less cost. In addition, due to the uniform heating, this method facilitates to generate smaller particles having narrow size distribution and phase with high purity.^{1,16}

Liu et al.⁴ found that Bi_2S_3 nanorods can serve as nanomedicine for *in-vivo* multimodal imaging-guided photothermal therapy of tumor. Further to utilize it as a nanomedical device, understanding their pharmacokinetics is needed but these results are still awaited. To understand their pharmacokinetics, the interaction of Bi_2S_3 nanorods with human serum albumin (HSA) has to be investigated since HSA transports the bioactive substances in the circulatory system as a carrier conjugate and the pharmacokinetics depends on the binding affinity of the bioactive substances with HSA.^{17,18} This *in-vitro* binding interaction between a bioactive substances and HSA can be easily identified using spectral methods. In particular, the fluorescence quenching technique stands as the most frequently used method to monitor the

^a Advanced Ceramics and Nanotechnology Laboratory, Department of Materials Engineering, University of Concepcion, Concepcion, Chile.

^b Nanomaterials & Solar Energy Conversion Lab, Department of Chemistry, National Institute of Technology, Tiruchirappalli 620015, India.

^c Department of Environmental Engineering and Science, Feng Chia University, Taichung 407, Taiwan.

^d The Center of Excellence for Advanced Materials Research, King Abdul Aziz University, Jeddah 21413, P.O. Box 80203, Saudi Arabia.

† Corresponding Authors

* (R.V.M) E-mail: mangal@udec.cl; Tel.: +56 41 2207389; fax: +56 41 2203391.

** (S.A) E-mail: sanand@nitt.edu, sanand99@yahoo.com; Tel.: +91 431 2503639; fax: +91 431 2500133.

molecular interactions because of its high sensitivity, reproducibility, and relatively very easy.¹⁹

HSA is the most abundant extracellular protein in the circulatory system of human body which not only transports endogenous as well as exogenous compounds and a variety of pharmaceuticals but also regulates the colloidal osmotic pressure of blood.^{20,21} While binding with a bioactive substances, it increases the solubility and reduces the toxicity of the bioactive substance along with protecting the bound bioactive substance against oxidation.¹⁸ It is synthesized by human liver and their half-life is approximately 19 days. It is a heart shaped molecule consisting of a single non-glycosylated polypeptide chain having 585 amino acid residues restrained by disulfide bridges, with a molecular weight of about 66.438 kDa.^{21,22} It constitutes of three homologous alpha-helical domains I (1–195), II (196–383) and III (384–585), that are packed in two separate sub-domains A and B which contain six and four α -helices, respectively.^{21,23} According to Sudlow's nomenclature, it has two principal binding sites namely Sudlow's I and II sites that are located in subdomain IIA and IIIA, respectively.²¹

The aim of this work is to study the interaction of Bi₂S₃ nanorods with HSA (Fig. 1a) for assessing their binding characteristics to understand their pharmacokinetics. In this regard, Bi₂S₃ nanorods were successfully synthesized by simple microwave irradiation method using bismuth nitrate and sodium sulfide as Bismuth and Sulfur source respectively along with starch as stabilizing agent. The interaction of this microwave synthesized Bi₂S₃ nanorods with HSA was investigated using different spectroscopic methods such as UV-vis spectroscopy, fluorescence and circular dichroism (CD). On the basis of the spectroscopic data, the quenching mechanism, binding constant, the number of binding sites, the binding site and the energy transfer process distance of HSA-Bi₂S₃ nanorods were calculated. Further, the secondary and tertiary structural changes occurred in the HSA on binding with Bi₂S₃ nanorods were estimated using CD spectral analysis. Thus obtained results may have significant applications in nanomedical device designing.

2. Materials and Methods

2.1 Materials

Bismuth nitrate pentahydrate Bi(NO₃)₃·5H₂O, sodium sulfide nonahydrate Na₂S·9H₂O, and HSA were purchased from Sigma-Aldrich. All other reagents used were of analytical reagent grade and used without any further purification. Water from a Milli Q system apparatus (Millipore, USA) was used throughout the experiments.

2.2 Methods

2.2.1 Microwave Assisted Synthesis of Bi₂S₃ Nanorods

Bi(NO₃)₃·5H₂O (10 mM) and starch (1 wt%) were dissolved in 25 ml of water taken in a round-bottomed flask. Under stirring, aqueous Na₂S·9H₂O (15 mM, 25 ml) solution was added drop wise to the round-bottomed flask and this mixture was heated for 10 min in a domestic cooking microwave oven (2450 MHz,

Whirlpool) with a refluxing apparatus circulated with ice-cold water. Thus formed black precipitate was centrifuged, washed several times with distilled water and ethanol, then dried in vacuum at 60°C and collected for further characterization.

2.2.2 Interaction studies

HSA solution was prepared in pH 7.4 phosphate buffer solution and stored at 0–4°C. HSA concentration was kept fixed at 4 μ M and the concentration of Bi₂S₃ nanorods has been varied from 0 to 4 μ M. This mixture has been sonicated in an ultrasonic bath for 1 minute in order to make serum albumins and Bi₂S₃ nanorods to combine completely. This titration has been monitored using steady-state fluorescence, time-resolved fluorescence and UV-vis absorption spectroscopy. For synchronous fluorescence spectroscopy and circular dichroism technique, HSA concentration was maintained at 4 μ M in the absence (0 μ M) and presence (4 μ M) of Bi₂S₃ nanorods.

2.3. Instrumentation

The Bi₂S₃ nanorods were characterized by powder X-ray diffraction (XRD), high-resolution transmission electron microscopy (HRTEM), selected area electron diffraction (SAED), and energy-dispersive X-ray (EDX). XRD spectra were recorded with a Philips PW1710 diffractometer using Ni filtered Cu radiation. The sample was allowed to equilibrate with atmospheric moisture for at least 24 hours prior to recording. The scanning range was 10–80 degrees (2 θ) with a step of 0.02 degrees and a count time of 2 seconds. TEM images along with SAED pattern and EDX spectrum were micrographed in TECNAI G² model in which samples were coated on copper grid at normal atmospheric temperature and pressure.

The interaction was investigated using UV-vis absorption spectroscopy, fluorescence spectroscopy, synchronous fluorescence spectroscopy and circular dichroism spectroscopy. UV-vis absorption spectra were recorded on T90+ UV-vis spectrophotometer (PG Instruments, United Kingdom) with 1.0 cm quartz cell. Fluorescence spectroscopy measurements were performed on RF-5301 PC spectrofluorophotometer (SCHIMADZU, Japan) using a 1.0 cm quartz cell. Excitation and emission slit widths of 5 nm were constantly retained for fluorescence studies. The scan speed was maintained at 240 nm min⁻¹. The samples were cautiously degassed using pure nitrogen gas for 15 minutes before doing every experiment. Fluorescence lifetime measurements were carried out in a picosecond time correlated single photon counting (TCSPC) spectrometer with tunable Ti-sapphire laser (TSUNAMI, Spectra physics, USA) as the excitation source. The fluorescence decay curves were analyzed using the software provided by IBH (DAS-6). Circular dichroism (CD) spectra were recorded on a Jasco J-810 spectropolarimeter under constant nitrogen flush over a wavelength range of 190–270 nm at a scanning speed of 200 nm min⁻¹.

3. Results and discussion

3.1 Characterization of Bi₂S₃ nanorods

The phase crystallinity and purity of microwave synthesized Bi₂S₃ nanorods were confirmed by the powder XRD spectrum

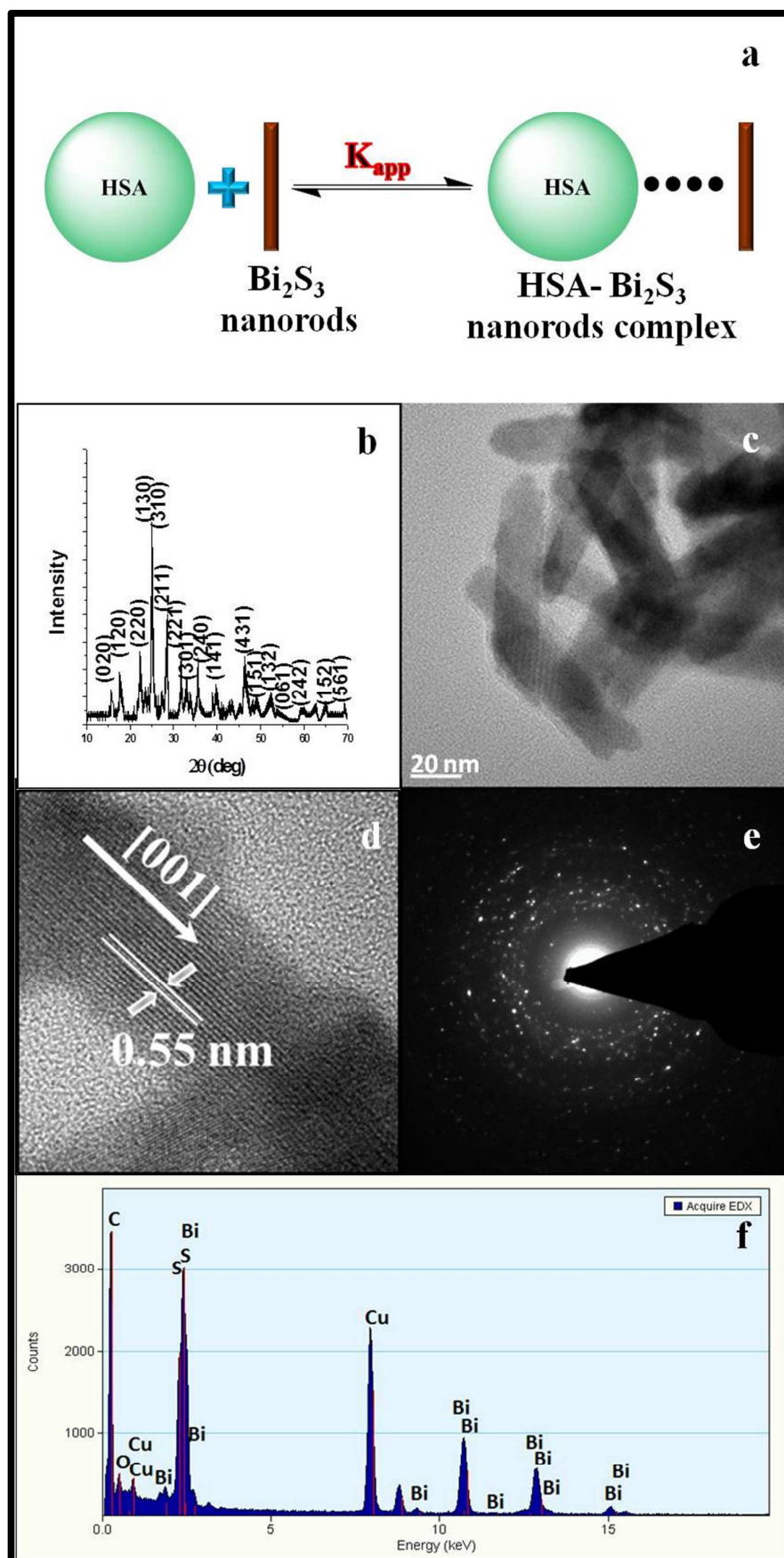


Fig. 1 (a) The interaction between HSA and Bi_2S_3 nanorods. XRD (b), TEM (c), HRTEM (d), SAED (e), and EDX (f) of Bi_2S_3 nanorods.

(Fig. 1b). All the diffraction peaks can be readily indexed to the orthorhombic Bi_2S_3 phase of the JCPDS database no. (17-0320). No other peaks were present which indicates the purity of Bi_2S_3 nanorods. The sharp diffraction peaks indicates that the products (Bi_2S_3) are well crystalline orthorhombic structure.¹

The morphology and composition of microwave synthesized Bi_2S_3 nanorods was characterized using transmission electron microscope. The TEM image (Fig. 1c) shows well-crystallized rod-like shaped particles with average dimensions of ca. 15 nm in width and 60-100 nm range in length. In addition, it showed the random distribution of Bi_2S_3 nanorods which can be attributed to the very fast growth of Bi_2S_3 in water medium.⁸ Slightly agglomerated particles were evident from the TEM image which may be due to the drying process of the sample preparation for TEM. High resolution TEM image (Fig. 1d) shows the lattice structure with the interplanar spaces of 0.55 nm in parallel with the nanorods, corresponding to the [2 0 0] crystallographic plane. The plane [2 0 0] is parallel to the growth direction, indicating that the nanorod tends to grow along the [0 0 1] direction.⁵ The SAED pattern of Bi_2S_3 nanorods, shown in Fig. 1e, revealed several diffraction rings, which is the sum of the diffraction pattern of different individual nanorods, indicating the polycrystalline nature.^{1,16} The energy dispersive X-ray (EDX) spectrum shown in Fig. 1f suggests that Bi and S were detected in the ratio of 38.5:61.5 which is nearly 2:3. The other peaks such as C and O are ascribed to the presence of starch which is used as the stabilizer whereas Cu arise from the copper grid used.

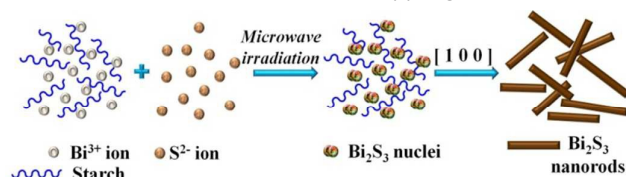


Fig. 2 The formation mechanism of Bi_2S_3 nanorods.

In this synthesis of Bi_2S_3 nanorods using microwave irradiation technique, starch has been utilized as the stabilizing agent because starch reduces the cytotoxicity of nanoparticles which arises from its biodegradable nature. In addition, starch has several advantages such as inexpensive, hydrophilic, non-toxic, biocompatible, and abundantly available.²⁴ The formation mechanism of Bi_2S_3 nanorods using $\text{Bi}(\text{NO}_3)_3$ and Na_2S in aqueous solution under microwave heating is proposed in Fig. 2. Under microwave irradiation, Bi^{3+} ions from $\text{Bi}(\text{NO}_3)_3$ react with S^{2-} ions from Na_2S to form Bi_2S_3 nuclei around long chain of starch. These freshly formed Bi_2S_3 nuclei in the solution are affected and controlled by starch to grow along the [0 0 1] direction into Bi_2S_3 nanorods.^{1,25,26}

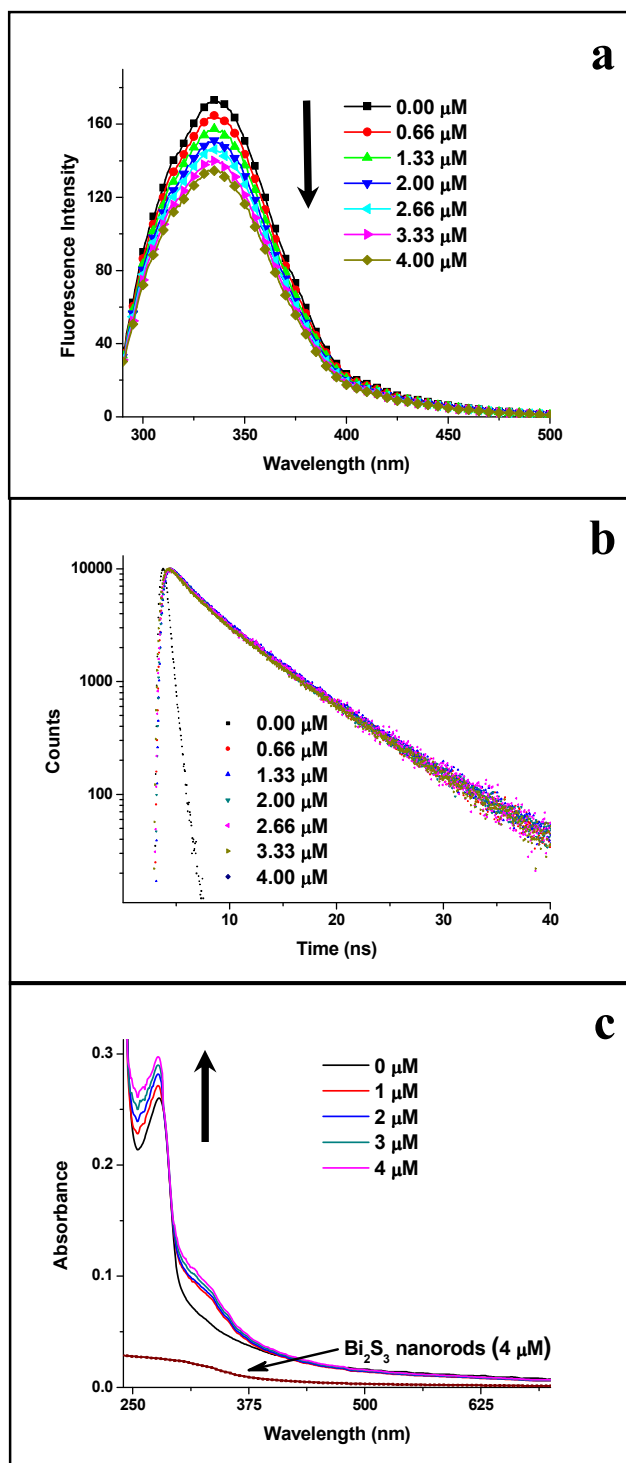
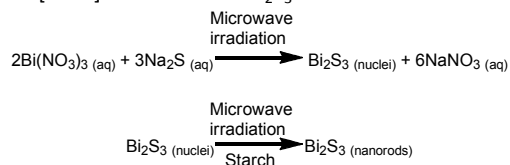


Fig. 3 Fluorescence spectra at $\lambda_{\text{ex}} = 280$ nm (a), Fluorescence decay curves (b) and absorption spectra (c) of HSA (4 μM) quenched by Bi_2S_3 nanorods in the concentration range of 0 - 4 μM . The absorbance of Bi_2S_3 nanorods (4 μM) at 280 nm found from the absorption spectrum (Fig. 3c) is 0.0257.

3.2 Interaction mechanism between HSA and Bi₂S₃ nanorods

In spite of having three intrinsic fluorophores such as tryptophan (Trp), tyrosine (Tyr) and phenyl alanine (Phe) in HSA, most of the fluorescence characteristic of HSA has been contributed by the Trp and Tyr residues because of the low fluorescence quantum efficiency of Phe. HSA has only one Trp residue at amino acid residue position 214 located in sub-domain IIA and 17 tyrosine residues.²⁷ Since the intrinsic fluorescence is very sensitive to the environmental changes,²² the fluorescence experiments were carried out in the absence and the presence of Bi₂S₃ nanorods (Fig. 3a). The fluorescence emission spectrum of HSA shows a strong fluorescence emission peak at 335 nm while exciting at 280 nm. While increasing the concentration of Bi₂S₃ nanorods from 0 to 4 μM, the fluorescence intensity of HSA decreases gradually along with blue shift in the emission maxima which indicates that Bi₂S₃ nanorods interact with HSA and quench its intrinsic fluorescence along with increasing the hydrophobicity of the fluorophore microenvironment.^{17,27}

The quenching mechanisms between the fluorophore and the quencher can be usually classified as either static or dynamic, in which static quenching is caused by the non-fluorescent ground state complex formation whereas dynamic quenching results from the collisional encounters. The static quenching mechanism can be distinguished from the dynamic quenching by their differing dependence on temperature and viscosity, absorption spectroscopy or preferably by the fluorescence lifetime measurements.^{17,18}

While considering the fluorescence lifetimes, the quencher will shorten the fluorescent lifetime of the excited molecules in dynamic quenching, but for static quenching, the quencher does not affect the fluorescence lifetime of the molecule.^{17,27,28} No remarkable change in the fluorescence lifetime decay of HSA is observed even on the addition of Bi₂S₃ nanorods (Fig. 3b) which confirms the static quenching mechanism takes place upon interaction of HSA with Bi₂S₃ nanorods.

Absorption spectroscopy is a simple, versatile and effective method for confirming the possible quenching mechanism. Static quenching influences the absorption spectra of the fluorophore whereas dynamic quenching influences only the fluorescence spectra.^{17,29} In this regard, the absorption spectra of 4 μM HSA with varying Bi₂S₃ nanorods concentration range of 0-4 μM were measured (Fig. 3c). While adding Bi₂S₃ nanorods, the absorption intensity increases with a blue shift in the maximum absorption wavelength of HSA around 278 nm which corresponds to the n→π* transition of peptide bond as well as the amino acid residues such as Trp, Tyr, and Phe of HSA. This blue shift indicates the interaction of HSA with Bi₂S₃ nanorods through a static quenching process i.e., ground state complex formation.^{17,18,28,29} Therefore, the equilibrium for the interaction of HSA with Bi₂S₃ nanorods represented in Fig. 1a, in which K_{app} represents the apparent association constant. This K_{app} can be obtained by means of the absorption intensity changes of the peak maxima using the following equation reported in literature:^{20,30}

$$\frac{1}{A_{obs} - A_0} = \frac{1}{A_{comp} - A_0} + \frac{1}{K_{app}(A_{comp} - A_0)[Bi_2S_3 \text{ nanorods}]} \quad (1)$$

where A_{obs} is the observed absorbance of the solution containing different concentrations of Bi₂S₃ nanorods at the peak maxima, A_0 is the absorbance of HSA, and A_{comp} is the absorbance of the complex at peak maxima, respectively. The value of the apparent association constant (K_{app}), determined from the linear relationship between $1/(A_{obs}-A_0)$ versus the reciprocal concentration of Bi₂S₃ nanorods (Fig. S1, Supporting information) with a slope equal to $1/[K_{app} \cdot (A_{comp}-A_0)]$ and an intercept equal to $1/(A_{comp}-A_0)$, was found to be $6.21 \times 10^4 \text{ M}^{-1}$.

Stern-Volmer equation²⁷ can also be used to recognize the quenching mechanism:

$$\frac{F_0}{F} = 1 + K_{SV}[Q] = 1 + K_q \tau_0 [Q] \quad (2)$$

where F_0 and F are the fluorescence intensities of serum albumins in the absence and presence of quencher; τ_0 is the average lifetime of the fluorophore (HSA) in the absence of quencher; K_{SV} , K_q and $[Q]$ are the Stern-Volmer quenching constant, bimolecular quenching rate constant (or the efficiency of quenching) and the quencher concentration respectively. HSA titrated by Bi₂S₃ nanorods shows a linear Stern-Volmer plot (Fig. S2, Supporting Information) with correlation coefficient $r = 0.9995$. From the slope of the linear plot, the Stern-Volmer quenching constant K_{SV} is found out to be $7.11 \times 10^4 \text{ M}^{-1}$. Since the lifetime of HSA, τ_0 , is found out to be $5.33 \times 10^{-9} \text{ s}$ from the fluorescence lifetime decay studies, bimolecular quenching rate constant K_q for the interaction of HSA with Bi₂S₃ nanorods is $1.33 \times 10^{13} \text{ M}^{-1} \cdot \text{s}^{-1}$ which is greater than the maximum scattering energy transfer between various quenchers and biopolymers collisional quenching ($2.0 \times 10^{10} \text{ M}^{-1} \cdot \text{s}^{-1}$) and this again suggests that static quenching mechanism was predominant in the interaction of HSA with Bi₂S₃ nanorods.

3.3 Binding constant and the binding site

The binding constant (K_A) of Bi₂S₃ nanorods with HSA and the number of binding sites (n) can be found using the Hill equation:

$$\log \left[\frac{F_0 - F}{F} \right] = \log K_A + n \log [Q] \quad (3)$$

From the intercept and the slope of the linear plot obtained in the double-logarithm regression curves of $\log[(F_0-F)/F]$ versus $\log[Q]$ (Fig. S3, Supporting Information), the values of K_A and n have been determined to be $3.55 \times 10^4 \text{ M}^{-1}$ and 0.9453. This value of n close to 1 indicates the presence of only one class of independent binding site in HSA for Bi₂S₃ nanorods which suggests the possible formation of 1:1 complex between HSA and Bi₂S₃ nanorods.^{31,32} This binding constant in the range of $1-15 \times 10^4 \text{ M}^{-1}$ suggests the moderate binding between HSA and Bi₂S₃ nanorods which can be attributed to the formation of less stable HSA-Bi₂S₃ nanorods complex. This binding constant K_A was further used to calculate the free energy change (ΔG°) using the equation

$$\Delta G^\circ = -RT \ln K_A \quad (4)$$

where R is the gas constant ($8.314 \text{ J}\cdot\text{mol}^{-1}\cdot\text{K}^{-1}$) and T is the temperature (298 K). At 298 K, the standard free energy change ΔG° was estimated to be $-2,334 \text{ J}\cdot\text{mol}^{-1}$ which indicates that the interaction of HSA with Bi_2S_3 nanorods was spontaneous.²⁷

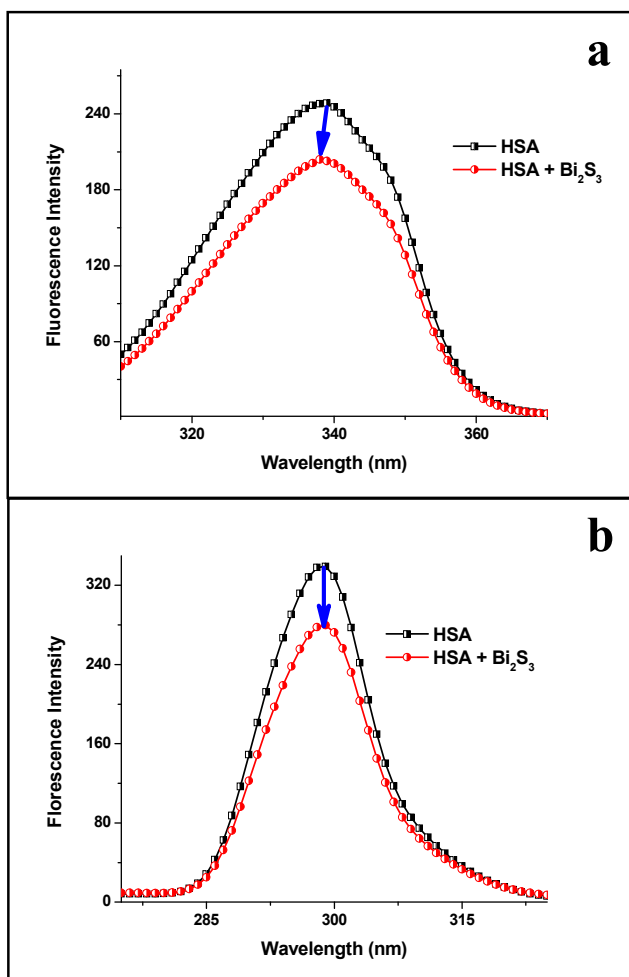


Fig. 4 Synchronous fluorescence spectra [(a) $\Delta\lambda = 60 \text{ nm}$ and (b) $\Delta\lambda = 15 \text{ nm}$] of HSA ($4 \mu\text{M}$) quenched by Bi_2S_3 nanorods in the concentration of 0 and $4 \mu\text{M}$.

Synchronous fluorescence spectra is a simple, selective and sensitive spectral method for providing the information on the molecular microenvironment in the vicinity of the fluorophore functional groups by synchronously scanning the excitation and emission monochromators while maintaining a constant wavelength interval ($\Delta\lambda$) between them. In HSA, the synchronous fluorescence will give information characteristic of Trp and Tyr residues by noticing the shift in the emission maximum (λ_{em}) when $\Delta\lambda$ is stabilized at 60 and 15 nm respectively.^{29,30} The effect of Bi_2S_3 nanorods on the synchronous spectra of HSA showed that the successive additions of Bi_2S_3 nanorods gradually decreased the intensity along with the slight blue shift when $\Delta\lambda$ is 60 nm (Fig. 4a)

whereas no shift was observed when $\Delta\lambda$ is 15 nm (Fig. 4b). This blue shift indicates the increase in the hydrophobicity of the microenvironment around the Trp residue on the addition of Bi_2S_3 nanorods resulting in the increase of hydrophobicity of the fluorophore environment.³³

3.4 Fluorescence resonance energy transfer

Förster theory of non-radiative energy transfer or fluorescence resonance energy transfer (FRET) can be used to calculate the distance ' r_0 ' between Bi_2S_3 nanorods and the Trp residue of HSA due to the good overlapping (Fig. S4, Supporting Information) between the absorption spectrum of acceptor (Bi_2S_3 nanorods) and the fluorescence spectrum of donor (HSA).³⁴ The energy transfer is related not only to the distance ' r_0 ' between the acceptor and donor, but also to the critical energy-transfer distance ' R_0 ' i.e., the critical distance when the transfer efficiency is 50%. Thus,

$$E = \frac{R_0^6}{R_0^6 + r_0^6} \quad (5)$$

where E is the energy transfer efficiency which can be determined experimentally from the fluorescence spectrum of donor with (F) and without (F_0) the acceptor concentration using the following equation^{17,27,28,34}

$$E = 1 - \frac{F}{F_0} \quad (6)$$

R_0 can be calculated using the equation

$$R_0^6 = 8.8 \times 10^{-25} k^2 N^{-4} \phi_D J \quad (7)$$

where k^2 is the spatial orientation factor related to the geometry of the donor and acceptor dipoles (2/3), N is the refractive index of the medium (1.336), ϕ_D is the fluorescence quantum yield of the donor (0.15) and J is the overlap integral of the fluorescence emission spectrum of the donor and the absorption spectrum of the acceptor.³⁵⁻³⁷ J can be calculated using the equation

$$J = \frac{\sum F(\lambda) \varepsilon(\lambda) \lambda^4 \Delta\lambda}{\sum F(\lambda) \Delta\lambda} \quad (8)$$

where $F(\lambda)$ is the fluorescence intensity of the donor at wavelength range λ to $\lambda + \Delta\lambda$ and $\varepsilon(\lambda)$ is the extinction coefficient of the acceptor at wavelength λ . Using the equations 5-8, the values of E, R_0 and r_0 has been found out to be 11.93%, 4.07 nm and 5.68 nm respectively. The donor to acceptor distance ' r_0 ' is less than 7 nm as well as within the range of $0.5R_0$ to $1.5R_0$ which indicates the efficient energy transfer from HSA to Bi_2S_3 nanorods.^{17,28-30,34-37}

3.5 Circular dichroism

CD spectroscopy is a very sensitive analytical technique to examine the secondary and tertiary structure of proteins while interacting with different molecules. The far-UV CD spectrum of HSA (Fig. 5a) shows two negative peaks around 208 and 222 nm which are attributed to $n \rightarrow \pi^*$ transition of the α -helical peptide bonds. A decrease in the intensity was observed upon the addition of Bi_2S_3 nanorods which indicates the decrease in

the α -helix of HSA. The CD results are expressed in terms of mean residue ellipticity (MRE) in $\text{deg.cm}^2.\text{dmol}^{-1}$ according to the following equation

$$MRE = \frac{\theta_{obs}}{C \times n \times l \times 10} \quad (9)$$

where θ_{obs} is the observed ellipticity in millidegrees, C is the molar concentration of the HSA, n is the number of amino acid residues in HSA (585), and l is the path length in centimeter.^{30,31} The α -helical content of HSA was calculated from the MRE value at 208 nm using the following equation:

$$\alpha - \text{helix} (\%) = \frac{-MRE_{208} - 4000}{33000 - 4000} \times 100 \quad (10)$$

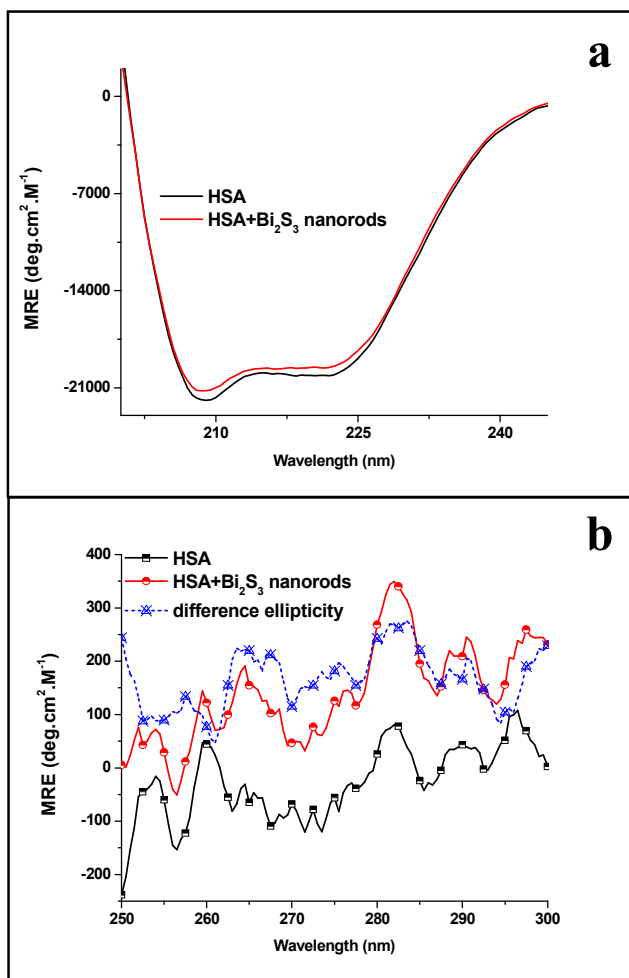


Fig. 5 Far UV (a) and near UV (b) circular dichroism spectra of HSA (4 μM) in the absence and presence of Bi_2S_3 nanorods (4 μM).

where MRE_{208} is the observed MRE value at 208 nm, 4000 is the MRE of the β -form and random-coil conformation cross at 208 nm, and 33,000 is the MRE of a pure α helix at 208 nm. Using the equations, the α -helix content in the secondary structure of HSA was determined to be 61.73% and 59.83% in the absence and presence of Bi_2S_3 nanorods. This decrease in the α -helix percentage indicates that Bi_2S_3 nanorods bound

with the amino acid residues of main polypeptide chain of HSA which causes slight unfolding of the polypeptide and leads to the conformational changes in HSA.^{17,29}

The tertiary structural changes can be investigated using the near-UV CD spectra of HSA in the absence and presence of Bi_2S_3 nanorods (Fig. 5b). The near-UV CD spectra of HSA shows two negative bands at 263 and 268 nm as well as two positive peaks at 275 and 290 nm which are characteristic of disulfide and the symmetric environment of aromatic amino acid residues. On the addition of Bi_2S_3 nanorods, the negative peaks at 262 and 268 nm as well as the positive peaks at 275 and 290 nm were significantly altered which indicates the partial disruption in the tertiary structure of HSA. The CD-spectral analysis showed that the overall conformation of HSA was disrupted in the presence of Bi_2S_3 nanorods.^{23,38,39} The difference ellipticity curve in Fig. 5b, the difference between the CD contribution of HSA in the presence and absence of Bi_2S_3 nanorods, displays negative extrema at 295 nm with less intense peaks between 270 and 290 nm. This observation again reveals that Bi_2S_3 nanorods interacts more with the tryptophan moiety than tyrosine moiety.^{40,41}

Conclusions

A simple microwave irradiation method was successfully employed to synthesize starch stabilized Bi_2S_3 nanorods which was then well characterized. XRD pattern along with HRTEM, and SAED images showed the formation of orthorhombic structured well crystalline Bi_2S_3 of ca. 15 nm in width with rod-like morphology. The binding characteristics of the microwave synthesized Bi_2S_3 nanorods with HSA were investigated using multispectroscopic techniques. The collective UV-vis and fluorescence (steady-state, time-resolved and synchronous) spectroscopic results determined that Bi_2S_3 nanorods bind spontaneously with HSA affecting the tryptophan moiety through static mechanism with a binding distance of 5.68 nm. CD spectral results suggests that HSA retained quite a lot of secondary structure as well as a significant proportion of tertiary structure while interacting with Bi_2S_3 nanorods. Knowledge on this interaction provides much valuable information that can be used for the better understanding on the design and applications of future nanomedical devices based on Bi_2S_3 nanorods.

Acknowledgements

The authors SN and RVM gratefully acknowledge the FONDECYT Post-doctoral Project No.: 3150102 and FONDECYT No.: 1130916, Government of Chile, Santiago, for the financial assistance. The authors SA and JJW thank Department of Science and Technology, India (GITA/DST/TWN/P-50/2013) and National Science Council (NSC), Taiwan (NSC-102-2923-035-001-MY3) respectively, for the India-Taiwan collaborative research grant.

References

- 1 T. Thongtem, A. Phuruangrat, S. Wannapop, and S. Thongtem, *Mater. Lett.*, 2010, **64**, 122.
- 2 A.J. MacLachlan, F.T.F. O'Mahony, A.L. Sudlow, M.S. Hill, K.C. Molloy, J. Nelson, and S.A. Haque, *ChemPhysChem*, 2014, **15**, 1019.
- 3 J. Fang, F. Chen, K.L. Stokes, J. He, J. Tang and C.J. O'Connor, *MRS Proceedings*, 2002, **730**, V5.5.1.
- 4 J. Liu, X. Zheng, L. Yan, L. Zhou, G. Tian, W. Yin, L. Wang, Y. Liu, Z. Hu, Z. Gu, C. Chen, and Y. Zhao, *ACS Nano*, 2015, **9**, 696.
- 5 J. Ma, J. Yang, L. Jiao, T. Wang, J. Lian, X. Duan, and W. Zheng, *Dalton Trans.*, 2011, **40**, 10100.
- 6 T. Wu, X. Zhou, H. Zhang, and X. Zhong, *Nano Res.*, 2010, **3**, 379.
- 7 R. Chen, M.H. So, C.-M. Che, and H. Sun, *J. Mater. Chem.*, 2005, **15**, 4540.
- 8 U.V. Kawade, R.P. Panmand, Y.A. Sethi, M.V. Kulkarni, S.K. Apte, S.D. Naik and B.B. Kale, *RSC Adv.*, 2014, **4**, 49295.
- 9 G. Nie, X. Lu, J. Lei, L. Yang, and C. Wang, *Electrochim. Acta*, 2015, **154**, 24.
- 10 M. Wang, H. Yin, N. Shen, Z. Xu, B. Sun, and S. Ai, *Biosensors Bioelectronics*, 2014, **53**, 232.
- 11 W. Zhang, Z. Yang, X. Huang, S. Zhang, W. Yu, Y. Qian, Y. Jia, G. Zhou, and L. Chen, *Solid State Comm.*, 2001, **119**, 143.
- 12 F. Wei, J. Zhang, L. Wang, and Z.K. Zhang, *Crys. Growth Des.*, 2006, **6**, 1942.
- 13 J.L.T. Chen, V. Nalla, G. Kannaiyan, V. Mamidala, W. Ji, and J.J. Vittal, *New J. Chem.*, 2014, **38**, 985.
- 14 Q. Han, Y. Sun, X. Wang, L. Chen, X. Yang, and L. Lu, *J. Alloys Compd.*, 2009, **481**, 520.
- 15 Q. Lu, F. Gao, and S. Komarneni, *J. Am. Chem. Soc.*, 2004, **126**, 54.
- 16 J. Wu, F. Qin, G. Cheng, H. Li, J. Zhang, Y. Xie, H.J. Yang, Z. Lu, X. Yu, and R. Chen, *J. Alloys Compd.*, 2011, **509**, 2116.
- 17 L.L. He, Y.X. Wang, X.X. Wu, X.P. Liu, X. Wang, B. Liu and X. Wang, *Lumin.*, 2015, doi: 10.1002/bio.2910
- 18 M. Saeidifar, and H.M. Torshizi, *Nucleosides Nucleotides Nucleic Acids*, 2015, **34**, 16.
- 19 S.D. Stojanovic, S.M. Jankovic, Z.D. Matovic, I.Z. Jakovljevic, and R.M. Jelic, *Monatsh. Chem.*, 2015, **146**, 399.
- 20 J. Yang, Y. Dong, L. Wang, D. Zhang, Z. Zhang, L. Zhang, *Sensors Actuators B*, 2015, **211**, 59.
- 21 A.M. Merlot, D.S. Kalinowski, and D.R. Richardson, *Front. Physiol.*, 2014, **5**, 299.
- 22 R. Yousefi, R. Mohammadi, A.T. Kafrani, M.B. Shahsavani, M.D. Aseman, S.M. Nabavizadeh, M. Rashidi, N. Poursasan, and A.A.M. Movahedi, *J. Lumin.*, 2015, **159**, 139.
- 23 X.X. Cheng, X.Y. Fan, F.L. Jiang, Y. Liu, and K.L. Lei, *Lumin.*, 2015 doi: 10.1002/bio.2854.
- 24 O.S. Oluwafemi and S.P. Songca, (2012) A Facile One-Pot Synthesis of MSe (M = Cd or Zn) Nanoparticles Using Biopolymer as Passivating Agent. Products and Applications of Biopolymers, Dr. Johan Verbeek (Ed.), ISBN: 978-953-51-0226-7, InTech, DOI: 10.5772/34186.
- 25 H.J. Kim, J. Park, K. Kim, M.K. Han, S.J. Kim, and W. Lee, *Chin. J. Chem.*, 2013, **31**, 752.
- 26 B. Xue, T. Sun, F. Mao, and J. Xie, *Mater. Lett.*, 2014, **122**, 106.
- 27 S. Naveenraj, and S. Anandan, *J. Photochem. Photobiol. C*, 2013, **14**, 53.
- 28 S. Naveenraj, S. Anandan, A. Kathiravan, R. Renganathan, and M. Ashokkumar, *J. Pharm. Biomed. Anal.*, 2010, **53**, 804.
- 29 L. Yang, J. Lv, X. Wang, J. Zhang, Q. Li, T. Zhang, Z. Zhang and L. Zhang, *J. Mol. Recognit.*, 2015, **28**, 459.
- 30 M.S. Ali, H.A. Al-Lohedan, A.M. Atta, A.O. Ezzat, S.A.A. Al-Hussain, *J. Mol. Liq.*, 2015, **204**, 248.
- 31 M.S. Ali, H.A. Al-Lohedan, A.M. Atta, A.O. Ezzat, S.A.A. Al-Hussain, *J. Mol. Liquids* 2015, **204**, 248.
- 32 S. Naveenraj, M.R. Raj, S. Anandan, *Dyes Pigm.* 2012, **94**, 330.
- 33 S. Naveenraj, A.M. Asiri, and S. Anandan, *J. Nanopart. Res.*, 2013, **15**, 1671.
- 34 J. Wang, Q. Wang, D. Wu, J. Yan, Y. Wu and H. Li, *Lumin.*, 2015, doi: 10.1002/bio.2921.
- 35 L. Kong, J. Hu, D. Qin, P. Yan, *J. Pharm. Innov.* 2015, **12**, 13.
- 36 Y. Li, Y. Zhang, S. Sun, A. Zhang, Y. Liu, *J. Photochem. Photobiol. B* 2013, **128**, 12.
- 37 X. Li, G. Wang, D. Chen, Y. Lu, *Food Chem.* 2015, **179**, 213.
- 38 M.T. Rehman, H. Shamsi, and A.U. Khan, *Mol. Pharm.* 2014, **11**, 1785.
- 39 S. Muzammil, Y. Kumar, and S. Tayyab, *Eur. J. Biochem.*, 1999, **266**, 26.
- 40 F. Zsila, *J. Phys. Chem. B* 2013, **117**, 10798.
- 41 S.M. Kelly, T.J. Jess, N.C. Price, *Biochim. Biophys. Acta* 2005, **1751**, 119.

Journal Name

ARTICLE

Insights into the binding of photothermal therapeutic agent bismuth sulfide nanorods with human serum albumin

Received 00th January 20xx,
Accepted 00th January 20xx

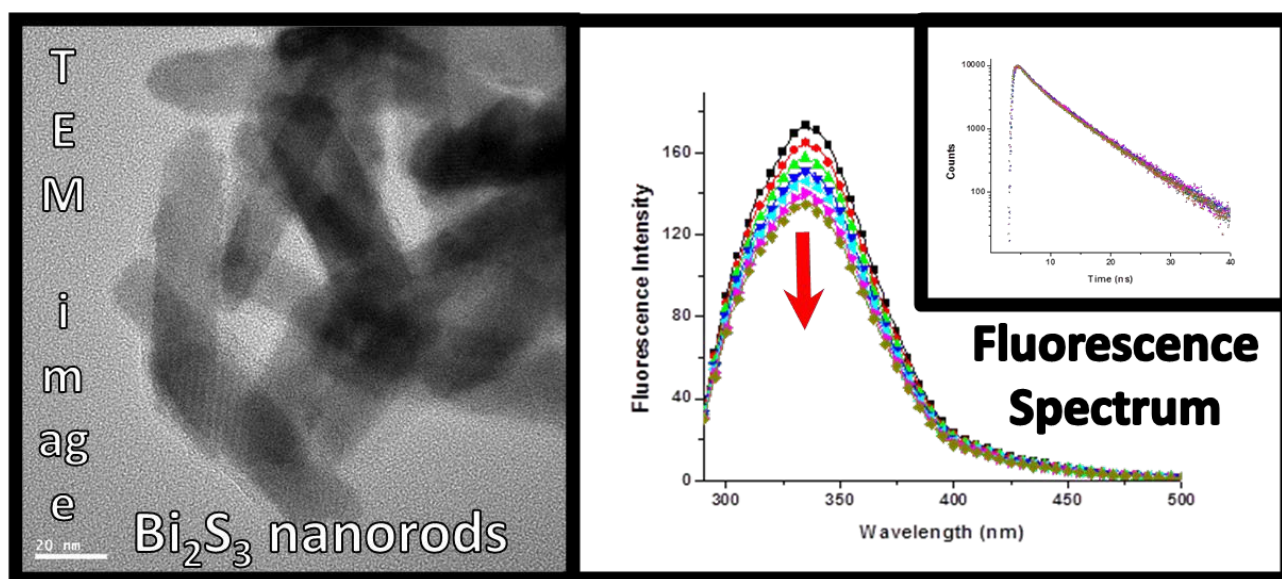
DOI: 10.1039/x0xx00000x

www.rsc.org/

Selvaraj Naveenraj^{a,b}, Ramalinga Viswanathan Mangalaraja^{a*}, Jerry J. Wu^c, Abdullah M. Asiri^d, Sambandam Anandan^{b**}

Starch stabilized Bismuth Sulfide nanorods were synthesized using microwave technique and their interaction with human serum albumin was investigated using multispectroscopic techniques such as absorption spectroscopy, fluorescence spectroscopy and circular dichroism spectroscopy.

Graphical Abstract



^aAdvanced Ceramics and Nanotechnology Laboratory, Department of Materials Engineering, University of Concepcion, Concepcion, Chile.

^bNanomaterials & Solar Energy Conversion Lab, Department of Chemistry, National Institute of Technology, Tiruchirappalli 620015, India.

^cDepartment of Environmental Engineering and Science, Feng Chia University, Taichung 407, Taiwan.

^dThe Center of Excellence for Advanced Materials Research, King Abdul Aziz University, Jeddah 21413, P.O. Box 80203, Saudi Arabia.

† Corresponding Authors

* (R.V.M) E-mail: mangal@udec.cl; Tel.: +56 41 2207389; fax: +56 41 2203391.

** (S.A) E-mail: sanand@nitt.edu, sanand99@yahoo.com; Tel.: +91 431 2503639; fax: +91 431 2500133.